processes

MDPI

Article

$Ca(OH)_2$-Modified White Mud Sorbent with Enhanced Performance for SO_2 Removal from Flue Gas

Hongyu Wang [1], Jianpeng Wei [1], Ye Wu [1], Chaohu Xiang [1], Li Yu [2], Lijian Jin [3], Wenrui Li [3,*], Hang Yu [3], Yitao Gan [3] and Danping Pan [4]

[1] Datang Environment Industry Group Co., Ltd., Beijing 100097, China
[2] East China Electric Power Test & Research Institute, China Datang Corporation Science and Technology General Research Institute Co., Ltd., Hefei 230061, China
[3] Key Laboratory of Energy Thermal Conversion and Control of Ministry Education, School of Energy and Environment, Southeast University, Nanjing 210096, China
[4] School of Environmental Engineering, Nanjing Institute of Technology, Nanjing 211167, China
* Correspondence: liwenruiseu@163.com; Tel.: +86-153-6572-8590

Abstract

The efficient utilization of industrial waste (containing alkaline compounds, especially Ca-based species) for flue gas desulfurization (FGD) is of great importance for both environmental protection and resource recovery. In this study, paper industry white mud was modified with $Ca(OH)_2$ to develop a cost-effective sorbent with enhanced SO_2 removal performance. Optimization experiments identified the best preparation conditions as a 1:1 $Ca(OH)_2$/white mud ratio, 60 °C modification temperature, 6 h reaction time, and a liquid-to-solid ratio of 3:1. Under these conditions, the sorbent achieved nearly 100% SO_2 removal in the first 6 h and maintained >90% efficiency after 10 h, significantly outperforming raw white mud and $Ca(OH)_2$ alone. Characterization revealed that the superior performance originated from structural stability and abundant active sites. BET analysis showed a high surface area (24.8 $m^2 \cdot g^{-1}$) and pore volume (0.160 $cm^3 \cdot g^{-1}$), which were largely preserved after desulfurization, indicating resistance to pore blockage. SEM images confirmed a transition from porous aggregates to densified product layers, consistent with a shrinking-core/product-layer mechanism. XRD identified $CaSO_4 \cdot 2H_2O$ as the dominant product, while in situ FTIR demonstrated that O_2 promotes sulfite oxidation and H_2O accelerates hydrated sulfate formation, enhancing activity but causing faster pore blocking. The presence of NO extended sorbent durability by catalyzing continuous sulfite oxidation through NO/NO_2 redox cycling. Overall, $Ca(OH)_2$-modified white mud combines high reactivity, durability, and structural stability, offering a promising alternative to conventional sorbents. This work provides a viable route for the resource utilization of paper industry waste and practical insights for designing efficient and sustainable materials for industrial FGD systems.

Keywords: white mud; $Ca(OH)_2$ modification; flue gas desulfurization (FGD); SO_2 capture; industrial waste valorization

Check for updates

Academic Editor: George Z. Kyzas

Received: 3 February 2026
Revised: 6 March 2026
Accepted: 23 March 2026
Published: 26 March 2026

Copyright: © 2026 by the authors. Licensee MDPI, Basel, Switzerland. This article is an open access article distributed under the terms and conditions of the Creative Commons Attribution (CC BY) license.

1. Introduction

With the rapid acceleration of industrialization, the combustion of large amounts of fossil fuels has led to a significant increase in sulfur dioxide (SO_2) concentrations in the atmosphere, resulting in severe environmental issues such as acid rain and haze, which pose serious threats to ecosystems and human health [1–3]. Flue gas desulfurization (FGD)

technology has been widely recognized as a key strategy for controlling SO_2 emissions and is extensively applied in power generation, steel, and cement industries [4–6]. Among various FGD techniques, calcium-based wet scrubbing remains dominant due to its low operational cost, high desulfurization efficiency, and operational stability [6–8]. However, conventional calcium-based sorbents suffer from substantial consumption of calcium resources and challenges associated with the effective utilization of by-products. Therefore, the development of economical, efficient, and resource-recoverable calcium-based sorbents has become a critical research focus in the field of flue gas desulfurization.

White mud, a typical solid waste generated from the paper industry [9–11], is primarily composed of calcium carbonate ($CaCO_3$) and contains a certain amount of active components such as calcium hydroxide ($Ca(OH)_2$) and magnesium hydroxide ($Mg(OH)_2$). Compared with conventional limestone-based sorbents, white mud slurry exhibits a higher pH (~12) [12,13], which is favorable for the efficient absorption of SO_2, while its active components further enhance the reaction activity [10,14–17]. Additionally, the fine particle size of white mud provides a large specific surface area, facilitating $CaCO_3$ dissolution and ionization [18–22]. Despite these advantages, unmodified white mud still suffers from insufficient reactivity and slurry clogging in practical applications, which significantly limits its large-scale utilization.

Recently, research on $Ca(OH)_2$-modified sorbents has attracted increasing attention [2,23–26]. For instance, causticization combined with thermal treatment can significantly reduce white mud particle size and increase surface area, thereby improving desulfurization performance. The incorporation of $Ca(OH)_2$ with catalysts in wet FGD systems has been shown to achieve SO_2 removal efficiencies exceeding 99%, while simultaneously enhancing sulfide oxidation and scaling resistance. Moreover, $Ca(OH)_2$ combined with fly ash in dry FGD systems has achieved high desulfurization rates in circulating fluidized beds. In addition, $Ca(OH)_2$–amorphous SiO_2 composites forming C–S–H phases have demonstrated superior desulfurization performance. Nevertheless, existing studies primarily focus on the combination of $Ca(OH)_2$ with single waste materials or catalysts, and systematic investigations on the synergistic modification of paper-industry white mud with $Ca(OH)_2$ remain limited.

Therefore, the aim of this work is to develop a cost-effective Ca-based sorbent by modifying paper-industry white mud with $Ca(OH)_2$ for flue gas desulfurization. Specifically, the preparation conditions are optimized in terms of $Ca(OH)_2$-to-white mud ratio, modification temperature, treatment time, and liquid-to-solid ratio. The SO_2-removal performance and durability are evaluated in fixed-bed tests, and the effects of key flue-gas components are examined. Finally, the structure–performance relationship and the desulfurization mechanism are elucidated using complementary characterizations, with emphasis on product-layer evolution and sulphur mineralization on the sorbent surface. The findings of this study not only provide a new pathway for the resourceful utilization of industrial white mud but also offer novel technical support for the sustainable development of sorbents and environmental protection, with significant theoretical and practical implications.

2. Experimental Section

2.1. Materials and Instruments

Paper-industry white mud was obtained from a commercial kraft pulp and paper mill located in Nanjing, China. To ensure homogeneity and reproducibility, the samples were first dried at 105 °C for 24 h, followed by ball milling and sieving through a 0.074 mm standard mesh. Analytical-grade calcium hydroxide ($Ca(OH)_2$) was used as the modifying agent, and deionized water was employed throughout the experiments. The experimental

setup comprised a thermostatic water bath, vacuum drying oven, mechanical stirrer, laboratory extruder, analytical balance, and glassware. The flue gas desulfurization (FGD) test system included a computer-controlled gas mixing unit, a temperature-controlled reaction tower, and an online flue gas analyzer for real-time monitoring.

Comprehensive characterization of the modified white mud sorbents was performed using the following techniques: (1) Surface area and porosity analysis: Brunauer–Emmett–Teller (BET) nitrogen adsorption was used to determine specific surface area, pore volume, and pore size distribution; (2) Crystalline structure analysis: X-ray diffraction (XRD) was conducted to identify the phase composition and crystalline characteristics of the modified sorbents; (3) Morphology observation: Scanning electron microscopy (SEM) was employed to examine particle surface morphology and pore structures; (4) Functional group analysis: In situ Fourier-transform infrared spectroscopy (FTIR) was applied to investigate the adsorption mechanism of SO_2 on the sorbent surface. Prior to each test, the sorbent was pretreated in a helium stream at 673 K for 1 h. The system was then cooled to 623 K and a background spectrum was collected after temperature stabilization. Subsequently, the desired reaction gas was introduced and time-resolved spectra were recorded immediately after gas switching at an interval of 30 s per spectrum for a total duration of 30 min (or until the signals reached a steady state).

2.2. Preparation of $Ca(OH)_2$-Modified White Mud

$Ca(OH)_2$ and dried white mud were thoroughly mixed at predetermined mass ratios ($Ca(OH)_2$:white mud, *w*/*w*) of 1:0, 0:1, 1:0.5, 1:1, 1:2, and 1:3. Deionized water was then added according to a solid-to-liquid ratio to form a homogeneous slurry. The slurry was sealed and subjected to thermal modification in a thermostatic water bath at 20–100 °C for 2–10 h. Continuous stirring was applied to ensure uniform reaction and prevent sedimentation or agglomeration.

After modification, the slurry was filtered to recover the solid product, which was subsequently dried in a vacuum oven at 120 °C until the moisture content was reduced to approximately 20%. After thermal modification, the samples were cooled to room temperature in a closed container and then stored in a desiccator/sealed bottle to minimize carbonation by ambient CO_2, yielding the $Ca(OH)_2$-modified white mud sorbent. Optimization of the modification process was achieved by varying $Ca(OH)_2$ content, treatment temperature, and reaction time.

2.3. Desulfurization Test Conditions and Evaluation

Desulfurization performance was evaluated using simulated flue gas containing SO_2, with high-purity N_2 (99.99%) as the carrier gas. A computer-controlled gas mixing system ensured uniform blending of SO_2, O_2, and N_2 at predetermined concentrations. The total gas flow rate was maintained at 2 L/min, with an SO_2 concentration of approximately 500 mg/m^3. In each experiment, 100 g of the modified white mud was loaded into the desulfurization reactor, and the reaction temperature was maintained at 120 °C. The SO_2 concentration in the inlet and outlet streams was continuously monitored using a portable flue gas analyzer (Testo 350, Testo SE & Co. KGaA, Germany). The SO_2 measurement range was 0–5000 ppm, and the accuracy was ±3%. The SO_2 removal efficiency was calculated using the following equation:

$$\text{SO}_2 \text{ removal efficiency}(\%) = \frac{C_{in} - C_{out}}{C_{in}} \times 100\% \quad (1)$$

where C_{in} and C_{out} represent the SO_2 concentrations at the reactor inlet and outlet, respectively (mg/m^3).

3. Results and Discussion

3.1. Physicochemical Properties of the Samples

The CaO content reported was obtained from bulk chemical analysis by X-ray fluorescence (XRF). Briefly, the dried and finely ground samples were analyzed by XRF, and the results were reported as oxide-equivalent mass fractions (ω, %) using the instrument's standard quantification and matrix correction; thus, CaO corresponds to total Ca expressed as CaO (stoichiometric conversion). Regarding Cl, it was identified and quantified simultaneously by XRF and is reported as elemental chlorine (Cl, wt%). Table 1 compares the chemical compositions of white mud and limestone. Both materials are predominantly composed of CaO, accounting for 92% and 96.8%, respectively, confirming that white mud possesses the fundamental characteristics of a calcium-based sorbent. Distinctly, white mud exhibits higher contents of Na_2O, MgO, SiO_2, and K_2O, which can improve slurry alkalinity, increase specific surface area, and enhance reactivity. Among them, MgO can directly participate in SO_2 capture, while SiO_2 and Al_2O_3 contribute to structural stability. Notably, the Cl content in white mud is markedly higher than in limestone, suggesting that part of the calcium may exist as $CaCl_2$, thereby facilitating calcium dissolution and accelerating SO_2 absorption. Overall, white mud not only supplies abundant reactive calcium species but also benefits from the synergistic effects of Mg, Si, and Al components, highlighting its technical feasibility and superior potential over limestone in flue gas desulfurization as well as resource utilization.

Table 1. Chemical compositions of white mud and limestone.

Composition (ω, %)	Samples	
	White Mud	Limestone
Na_2O	2.65	2.45
MgO	1.62	0.2
Al_2O_3	0.4	0.25
SiO_2	2.15	0.35
SO_3	0.11	0.03
K_2O	0.29	0.02
CaO	92	96.8
MnO	0.03	0.02
CuO	0.008	0.005
Cl	0.2	0.04

In addition to chemical composition, particle size distribution plays a crucial role in determining sorbent reactivity. As shown in Table 2, white mud exhibits significantly finer particles (D_{10} = 2.35 μm, D_{50} = 11.90 μm, D_{90} = 32.50 μm) compared with limestone (D_{10} = 4.50 μm, D_{50} = 70.20 μm, D_{90} = 450.00 μm). The narrow distribution of white mud particles results in a higher specific surface area and more uniform slurry dispersion, which facilitates rapid SO_2 dissolution and gas–solid contact during the reaction. By contrast, the coarse and broad particle size distribution of limestone limits surface availability and mass transfer efficiency, thereby reducing its intrinsic reactivity unless subjected to extensive grinding.

Table 2. Particle size distribution of white mud and limestone.

Samples	D_{10}/μm	D_{50}/μm	D_{90}/μm
White Mud	2.35	11.90	32.50
Limestone	4.50	70.20	450.00

Taken together, the combined advantages of chemical composition and particle size distribution highlight the technical feasibility of using white mud as a desulfurization sorbent. The presence of reactive calcium species, auxiliary metal oxides, and fine particle size distribution not only enhances SO_2 capture efficiency but also provides a cost-effective pathway for the resource utilization of industrial solid waste. Therefore, white mud demonstrates substantial potential as a sustainable substitute for conventional limestone in flue gas desulfurization applications.

3.2. Effect of Raw Material Ratio on Desulfurization Efficiency

Under the thermal modification conditions (reaction time 6 h, temperature 120 °C, and liquid-to-solid ratio 3:1), the influence of $Ca(OH)_2$-to-white mud ratios on desulfurization performance was investigated, as shown in Figure 1. When white mud was used alone, the SO_2 removal efficiency rapidly decreased with time, falling below 30% after 10 h, indicating limited active components and poor sorbent durability. In contrast, pure $Ca(OH)_2$ initially exhibited high desulfurization efficiency, but the efficiency decreased to ~65% after 10 h, reflecting insufficient long-term stability. The blended sorbents demonstrated a remarkable improvement in both efficiency and stability. At a $Ca(OH)_2$/white mud ratio of 1:1, the SO_2 removal efficiency remained nearly 100% within the first 6 h and was still above 90% after 10 h, representing the best overall performance. At a ratio of 1:2, the efficiency remained around 85% after 10 h, which was still superior to either raw material alone. However, when the ratio decreased to 1:3, the desulfurization efficiency significantly declined. These results suggest that the appropriate incorporation of $Ca(OH)_2$ enhances the reactivity and durability of white mud, with an optimal synergistic effect observed at the 1:1 mass ratio.

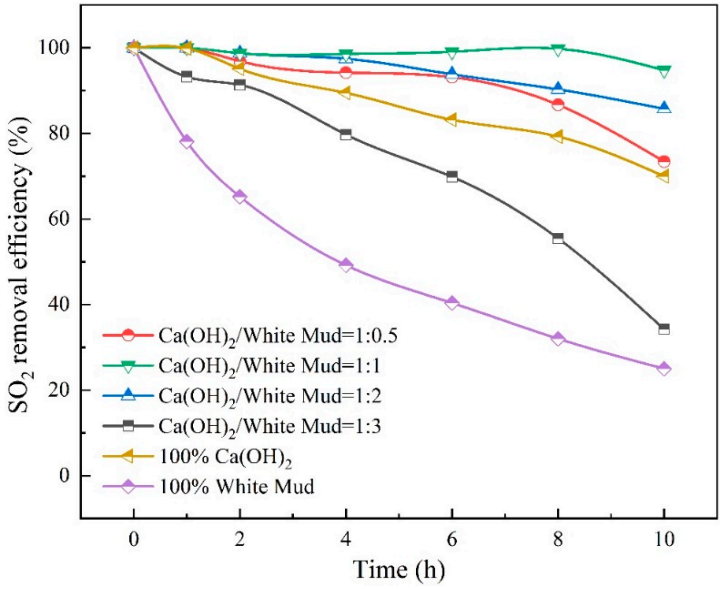


Figure 1. Effect of raw material ratio on desulfurization efficiency.

3.3. Effect of Thermal Modification Temperature on Desulfurization Efficiency

The effect of thermal modification temperature on the SO_2 removal performance of $Ca(OH)_2$–white mud sorbents (mass ratio 1:1) was investigated, and the results are presented in Figure 2. The desulfurization efficiency exhibited strong dependence on the modification temperature. At 20 °C and 40 °C, the sorbents showed rapid efficiency decay, with SO_2 removal decreasing to 14.9% and 45.3% after 10 h, respectively. This indicates that low modification temperatures are insufficient to activate the interaction between $Ca(OH)_2$ and white mud, leading to incomplete modification and poor utilization of active calcium species. By contrast, sorbents modified at 60 °C and 80 °C demonstrated

significantly improved performance, maintaining efficiencies of 92.2% and 93.1% after 10 h, respectively. Such enhanced behavior can be attributed to better dispersion of $Ca(OH)_2$ and stronger integration with white mud particles at moderate temperatures, which generate more accessible active sites. Moreover, appropriate thermal input likely contributes to optimized surface area and pore structure, thereby improving mass transfer and adsorption capacity. When the modification temperature was further increased to 100 °C, the efficiency slightly decreased to 89.9%, which may be ascribed to structural collapse or sintering at excessive temperatures, reducing the number of reactive sites available for SO_2 capture. Therefore, thermal modification temperature is a critical factor governing the performance of $Ca(OH)_2$-modified white mud sorbents, with ~60 °C identified as the optimal condition that balances high initial activity with long-term stability.

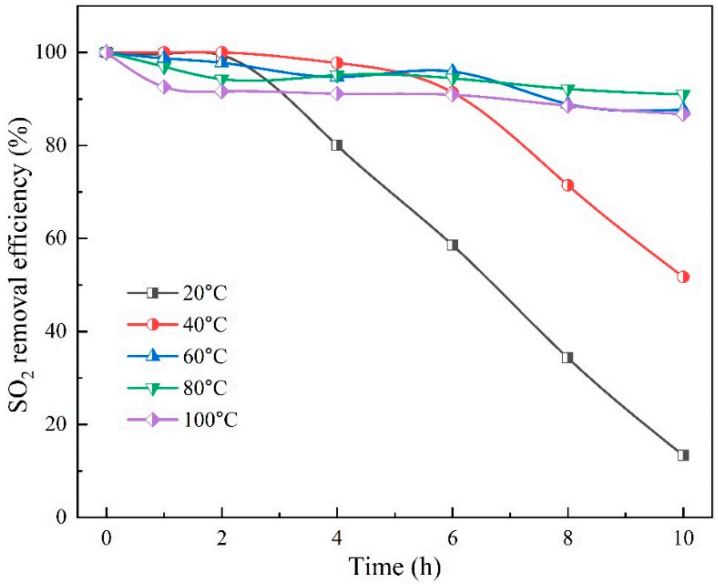


Figure 2. Effect of thermal modification temperature on desulfurization efficiency.

3.4. Effect of Thermal Modification Time on Desulfurization Efficiency

The effect of thermal modification time on the desulfurization performance of $Ca(OH)_2$–white mud sorbents (1:1 mass ratio) at 60 °C is shown in Figure 3. The results reveal that modification time exerts a pronounced influence on SO_2 removal efficiency. With insufficient modification (0.5 h and 1 h), the sorbents exhibited rapid efficiency decay, with final efficiencies of ~21% and ~38% after 10 h, respectively. This indicates incomplete formation of active sites and poor durability at short modification durations. At 2 h, the efficiency improved to 46.3%, but was still inadequate for practical desulfurization applications. When the modification time was extended to 4 h and 6 h, the desulfurization efficiency increased significantly, reaching 70.7% and 92.2% after 10 h, respectively. This enhancement can be attributed to the better dispersion of $Ca(OH)_2$ and its stronger interaction with white mud particles, generating more available active sites for SO_2 capture. However, further extension to 10 h resulted in only a marginal improvement (91.9%), suggesting that the modification process approached equilibrium, and prolonged treatment offered limited benefits. Overall, thermal modification time plays a crucial role in determining the performance of $Ca(OH)_2$-modified white mud sorbents. Moderate modification enhances surface area, pore structure, and reactivity, whereas insufficient treatment leads to poor performance and excessive treatment yields diminishing returns. Considering both performance and energy consumption, 6 h was identified as the optimal modification time.

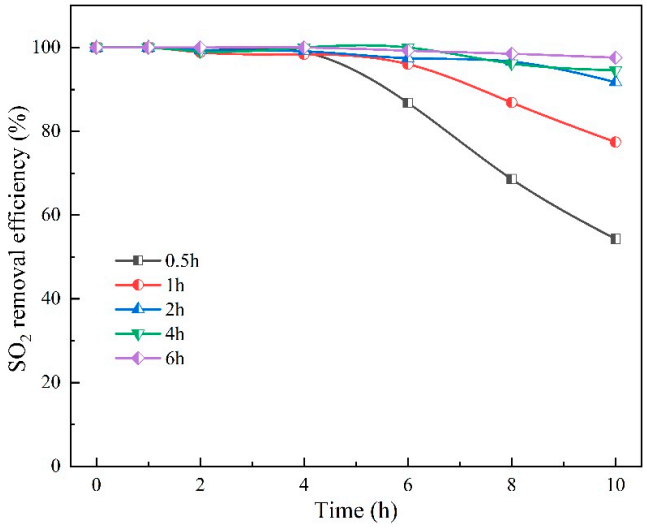


Figure 3. Effect of thermal modification time on desulfurization efficiency.

3.5. Effect of Liquid-to-Solid Ratio on Desulfurization Efficiency

The influence of liquid-to-solid ratio (L/S) on the desulfurization performance of $Ca(OH)_2$-modified white mud sorbents was investigated at 60 °C with a modification time of 6 h, as shown in Figure 4. The results demonstrate that the L/S ratio plays a critical role in determining sorbent activity. At an L/S ratio of 2:1, the SO_2 removal efficiency dropped rapidly to 32.6% after 10 h, suggesting that insufficient liquid hindered slurry dispersion and limited the contact between $Ca(OH)_2$ and white mud particles, thereby restricting the formation of active sites. When the L/S ratio was increased to 3:1, the sorbent exhibited the best performance, maintaining a high efficiency of 92.2% after 10 h. This indicates that a moderate L/S ratio ensures better mixing and uniform dispersion of $Ca(OH)_2$, resulting in more accessible active sites and enhanced SO_2 capture. However, further increasing the L/S ratio to 4:1, 5:1, and 6:1 led to decreased efficiencies of 75.5%, 66.5%, and 59.3%, respectively. The performance decline at higher L/S ratios may be attributed to overly diluted slurries, which reduce particle collision frequency and weaken the interaction between $Ca(OH)_2$ and white mud, thereby lowering modification effectiveness. Overall, the L/S ratio is a key parameter controlling the modification efficiency of white mud-based sorbents. Taking both desulfurization efficiency and energy consumption into account, an L/S ratio of 3:1 is identified as the optimal condition.

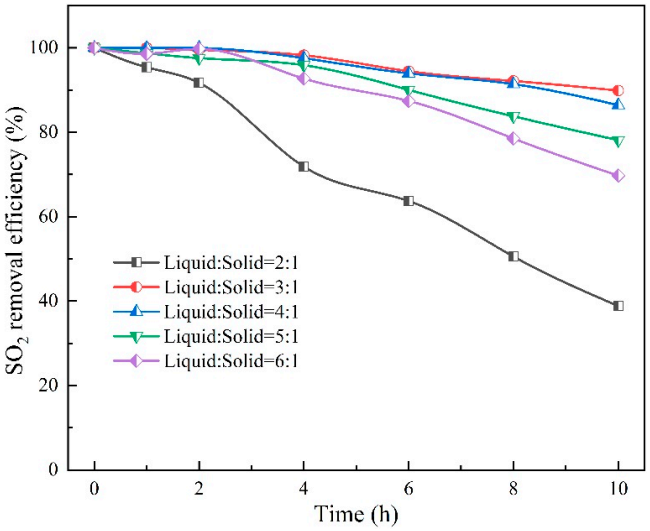


Figure 4. Effect of liquid-to-solid ratio on desulfurization efficiency.

3.6. Effect of Flue Gas Components on Desulfurization Efficiency

The influence of flue gas components on the desulfurization performance of $Ca(OH)_2$-modified white mud sorbents under optimized modification conditions is illustrated in Figure 5. All systems initially exhibited nearly 100% SO_2 removal efficiency, followed by different deactivation rates. In the SO_2-only atmosphere, the sorbent showed the fastest decline, dropping below 40% within 90 min and stabilizing at ~15–20% after 400 min, indicating rapid pore blockage and insufficient utilization of active calcium. The addition of water vapor slightly improved the initial reaction but significantly accelerated deactivation in the later stage, with efficiency declining to ~10–15%. This negative effect can be ascribed to the competitive adsorption of H_2O and the formation of hydrated sulfite/sulfate layers (e.g., $CaSO_3 \cdot ½H_2O$), which block pores and restrict SO_2 diffusion.

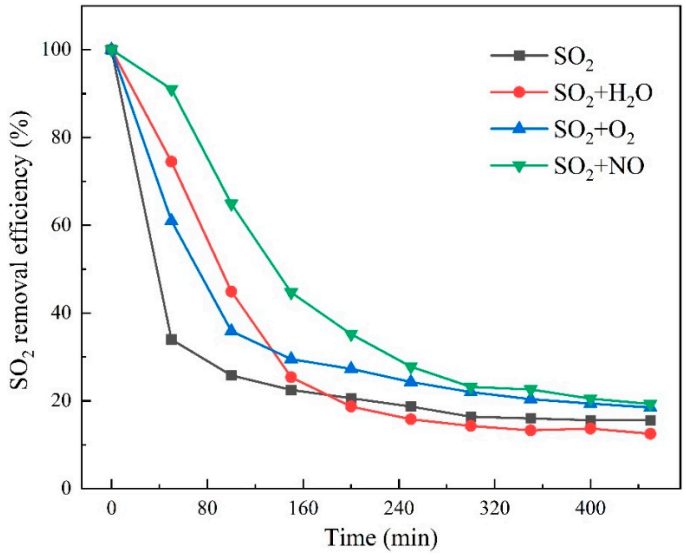


Figure 5. Effect of liquid-to-solid ratio on desulfurization efficiency.

In contrast, the presence of O_2 effectively enhanced desulfurization stability. The oxidation of sulfite to sulfate is thermodynamically favorable:

$$Ca(OH)_2 + SO_2 \rightarrow CaSO_3 + H_2O \quad (2)$$

$$CaSO_3 + \frac{1}{2}O_2 \rightarrow CaSO_4 \quad (3)$$

This pathway reduces the accumulation of $CaSO_3$, alleviates pore clogging, and prolongs sorbent lifetime. Consequently, SO_2 + O_2 maintained efficiencies of ~25–30% after 200 min and stabilized at ~18–20% in the long term.

The most pronounced improvement was observed in the SO_2 + NO atmosphere. The superior performance can be attributed to the redox cycling between NO and NO_2, which accelerates the oxidation of sulfite/bisulfite species to sulfate:

$$2NO + O_2 \rightarrow 2NO_2 \quad (4)$$

$$HSO_3^- + NO_2 \rightarrow SO_4^- + NO + H^+ \quad (5)$$

This catalytic cycle regenerates NO and sustains continuous sulfite oxidation, thereby suppressing the formation of diffusion-limiting sulfite layers and significantly extending the sorbent lifetime. A comparison of t_{50} (time required for efficiency to drop to 50%) further illustrates the differences: SO_2 ≈ 60–80 min; SO_2 + H_2O ≈ 100–140 min; SO_2 + O_2 ≈ 180–240 min; SO_2 + NO ≈ 220–300 min. Here, t_{50} is reported to compare deac-

tivation rates among gas atmospheres, while breakthrough/saturation times are defined based on outlet concentration criteria (e.g., $C/C_0 = 0.1$ for breakthrough and $C/C_0 = 0.95$ for saturation) to facilitate scale-up estimation; under the optimized condition, breakthrough was not reached within 10 h. These findings clearly demonstrate that while excess H_2O accelerates sorbent deactivation, the presence of O_2 and especially NO in flue gas promotes the formation of stable $CaSO_4$ and prolongs sorbent durability. Therefore, moderate O_2 and NO contents in flue gas are beneficial for maintaining high SO_2 removal efficiency, providing crucial guidance for the practical application of $Ca(OH)_2$-modified white mud sorbents in industrial flue gas desulfurization systems.

3.7. Desulfurization Mechanism of $Ca(OH)_2$-Modified White Mud

Figure 6 provides SEM evidence for the microstructural evolution of the $Ca(OH)_2$-modified white-mud sorbent during SO_2 capture. Fresh sorbents (Figure 6a,b) exhibit cauliflower-like aggregates built from sub-micrometer plates/grains with abundant inter-aggregate meso-/macropores. Such hierarchical porosity (macropores > 50 nm for bulk transport, mesopores 2–50 nm for diffusion/product accommodation, and micropores < 2 nm for high-energy adsorption), together with dense basic surface sites, enables rapid SO_2 uptake. After desulfurization (Figure 6c,d), pore mouths are progressively filled/bridged by reaction products and the surface becomes densified into a continuous product layer, occasionally with plate-like crystallites and micro-cracks, indicating a "formation–oxidation–densification" sequence. These features are fully consistent with the reaction pathway: initial chemisorption/neutralization of SO_2 on basic hydroxyls to form calcium sulfite, followed by oxidation to sulfate in the presence of O_2 and via the NO/NO_2 redox cycle. At non-negligible humidity, hydrated phases (e.g., $CaSO_3{\cdot}½H_2O/CaSO_4{\cdot}2H_2O$) may precipitate preferentially, first blocking micro/mesopores and then forming a continuous shell that raises intraparticle diffusion resistance, accounting for the observed decay in SO_2-removal efficiency from initially ~100%. In short, the $Ca(OH)_2$-modified white mud owes its high initial activity to hierarchical pore channels and basic sites, whereas the progressive accumulation and densification of (hydrated) sulfite/sulfate phases govern later-stage deactivation. In terms of kinetics, the sulphur mineralization rate on the sorbent surface is inherently time-dependent. At the initial stage, abundant basic sites and open pore mouths enable rapid neutralization/mineralization of SO_2, giving a high apparent rate. As Ca–S products accumulate, a porous product layer develops and gradually densifies, increasing intraparticle diffusion resistance; consequently, the mineralization rate decreases with time and progressively shifts from surface-reaction-dominated to mass-transfer-limited behavior, consistent with the porous product-layer shrinking-core mechanism evidenced by SEM densification and the later-stage decay in SO_2-removal efficiency. Practically, maintaining moderate O_2/NO (to accelerate $SO_3^{2-} \rightarrow SO_4^{2-}$ and yield a more permeable sulfate layer), controlling humidity (to avoid rapid hydrate-induced densification), and preserving mesoporosity via particle-size refinement and pore-stabilizing modification (e.g., SiO_2 scaffolding/templating, optimized thermal treatment) are effective to balance high initial efficiency with long service life.

Table 3 summarizes the BET results of fresh and used samples. Fresh white mud exhibits a very low specific surface area (6.7 $m^2{\cdot}g^{-1}$), pore volume (0.032 $cm^3{\cdot}g^{-1}$), and average pore diameter (19.1 nm), indicating limited adsorption capacity and explaining its poor desulfurization performance. By contrast, fresh $Ca(OH)_2$ shows higher values (16.0 $m^2{\cdot}g^{-1}$, 0.090 $cm^3{\cdot}g^{-1}$, 22.5 nm), leading to stronger SO_2 uptake. Notably, fresh $Ca(OH)_2$-modified white mud displays a markedly improved surface structure, with a specific surface area of 24.8 $m^2{\cdot}g^{-1}$, pore volume of 0.160 $cm^3{\cdot}g^{-1}$, and pore diameter of

25.8 nm. These results demonstrate that thermal modification effectively increases porosity and creates a hierarchical pore system, enhancing both SO_2 adsorption and product accommodation/diffusion. After desulfurization, both white mud and $Ca(OH)_2$ showed significant reductions in surface area (to 5.8 and 15.3 $m^2 \cdot g^{-1}$, respectively), accompanied by decreased pore volume and pore size, suggesting pore blocking by reaction products and reduced accessibility of active sites. In contrast, the used $Ca(OH)_2$-modified white mud maintained almost the same surface area (24.3 $m^2 \cdot g^{-1}$) and pore volume (0.150 $cm^3 \cdot g^{-1}$) as before the reaction, with only a slight reduction in pore size (25.5 nm). This remarkable structural stability indicates that the modified sorbent can effectively resist pore clogging, sustain gas diffusion into reactive regions, and thereby achieve higher Ca utilization and prolonged sorbent lifetime. In summary, BET analysis confirms that the superior desulfurization performance of $Ca(OH)_2$-modified white mud originates from its enhanced and stable pore structure, which simultaneously provides abundant adsorption sites and facilitates mass transfer throughout the desulfurization process.

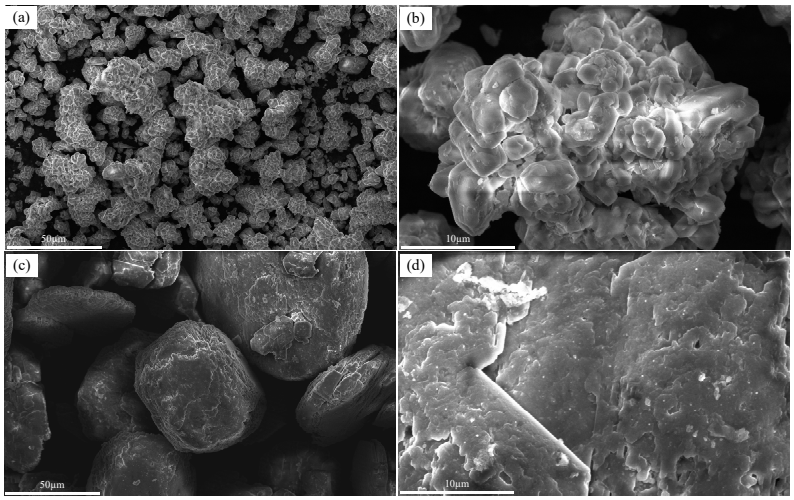


Figure 6. SEM images of (**a**,**b**) fresh white mud and (**c**,**d**) product after desulfurization.

Table 3. BET results of fresh and used samples.

Samples	Specific Surface Area/($m^2 \cdot g^{-1}$)	Pore Volume/($cm^3 \cdot g^{-1}$)	Pore Diameter/nm
Fresh white mud	6.7	0.032	19.1
Fresh $Ca(OH)_2$	16.0	0.090	22.5
Fresh $Ca(OH)_2$-modified white mud	24.8	0.160	25.8
Used white mud	5.8	0.027	18.4
Used $Ca(OH)_2$	15.3	0.082	21.0
Used $Ca(OH)_2$-modified white mud	24.3	0.150	25.5

Notably, the spent sorbent is expected to contain a mixture of residual Ca-bearing species (e.g., $CaCO_3$/$Ca(OH)_2$/CaO) and sulfur-containing products ($CaSO_3$ and $CaSO_4$). XRD is primarily used here to identify the dominant crystalline phases; however, it may not fully resolve poorly crystalline/amorphous or surface-enriched sulfite/sulfate species. As shown in Figure 7a, the fresh white mud is dominated by calcite $CaCO_3$ (PDF#81-2027) with minor CaO (PDF#28-0775). The slightly undulated background suggests the presence of amorphous silico-aluminate phases, consistent with the chemical analysis, yet their low content precludes resolvable peaks. This indicates that thermal modification primarily optimizes pore architecture and dispersion rather than creating new bulk phases—fully consistent with the BET (increased surface area and pore volume) and SEM (hierarchical

porosity) results. After desulfurization (Figure 7b), the diffraction pattern matches gypsum $CaSO_4 \cdot 2H_2O$ (PDF#33-0311), implying that surface sulfite formed during SO_2 capture was subsequently oxidized and hydrated to sulfate under O_2/NO-containing flue gas and during post-exposure to moisture. Besides gypsum, a few weak reflections likely originate from residual $CaCO_3$ and trace $CaO/Ca(OH)_2$ remaining from incomplete conversion of the Ca-based sorbent. Therefore, the conclusion on sulfate-dominated mineralization is supported by the combined evidence from XRD (phase identification), in situ FTIR (sulfite-to-sulfate evolution), and SEM/BET (product-layer formation and mass-transfer limitation), rather than relying on XRD alone. The absence (or weakness) of crystalline $CaSO_3$ reflections can be rationalized by (i) rapid oxidation/hydration driving sulfate as the thermodynamically favored end phase, and/or (ii) low crystallinity/low abundance of sulfite with peak overlap by gypsum. If a faint $CaCO_3$ peak around $2\theta \approx 29$–30° is still discernible, it evidences a shrinking-core/product-layer scenario: a sulfate shell forms outside while a calcite core remains, with further conversion limited by intraparticle diffusion. Taken together, XRD, SEM, and BET converge to a coherent mechanism: the high performance of $Ca(OH)_2$-modified white mud stems from basic active sites combined with a stable hierarchical pore network, whereas deactivation arises from the progressive deposition and densification of (hydrated) sulfate layers at pore mouths and surfaces. Accordingly, process control should mitigate rapid hydrate-induced densification (humidity management), exploit moderate O_2/NO to promote sulfite→sulfate conversion with more permeable layers, and preserve mesoporosity via modification to balance high initial activity and durability. Quantitative differentiation of surface vs. bulk sulfur speciation (e.g., sulfite versus sulfate fractions) would benefit from complementary techniques such as XPS and bulk elemental analysis (e.g., ICP-OES/ICP-MS), which will be incorporated in future work. As regeneration and end-of-life considerations, unlike regenerable sorbents governed by reversible adsorption, the present Ca-based sorbent captures SO_2 predominantly through mineralization into sparingly soluble and thermodynamically stable sulfate/hydrated sulfate (mainly $CaSO_4 \cdot 2H_2O$, as evidenced by XRD together with the sulfate-band growth in in situ FTIR). Therefore, full chemical regeneration back to $Ca(OH)_2/CaCO_3$ is not expected to be energy- or cost-effective under typical FGD conditions. From a practical perspective, the sustainability of this sorbent is better realized by: (i) maximizing Ca utilization enabled by the stable hierarchical pore structure (BET retention after reaction), (ii) partial physical reactivation (e.g., attrition/milling) to expose unreacted cores if a shrinking-core structure remains, and (iii) valorization of the spent sorbent as a gypsum-rich byproduct (e.g., for cement set regulation or gypsum-based materials), thereby closing the material loop. Systematic cyclic-use tests and byproduct-quality evaluation will be addressed in future work.

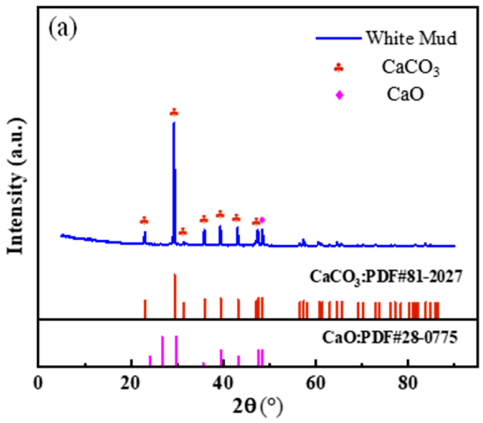


Figure 7. *Cont.*

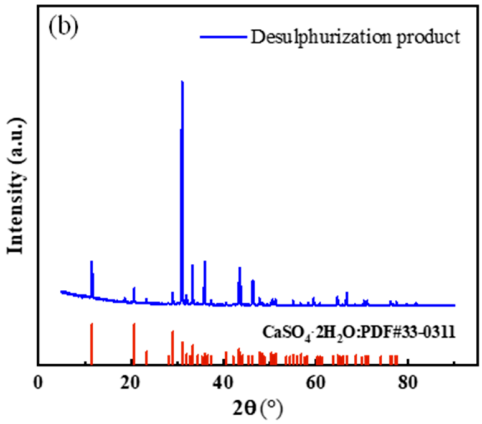


Figure 7. XRD images of (**a**) fresh white mud and (**b**) product after desulfurization.

To further investigate the effects of H_2O and O_2 on the desulfurization products and reaction mechanism, in situ infrared experiments were conducted under three different atmospheres: SO_2 alone, $SO_2 + O_2$, and $SO_2 + O_2 + H_2O$. The resulting steady-state spectra are shown in Figure 8a. Two atmosphere-dependent bands emerge in the 1200–1100 cm^{-1} region with maxima at 1189 cm^{-1} and 1128 cm^{-1}. The former is assigned to the asymmetric stretching $\nu_3(SO_4^{2-})$ of surface sulfate species, while the latter likely reflects either splitting due to different coordination/hydration states (e.g., $CaSO_4$ vs. $CaSO_4 \cdot 2H_2O$) or a minor contribution from surface sulfite/bisulfite complexes (SO_3^{2-}/HSO_3^-). Band intensities follow the order $SO_2 + O_2 + H_2O > SO_2 + O_2 > SO_2$, indicating that O_2 promotes the oxidation of sulfite to sulfate, and H_2O further amplifies sulfate—particularly hydrated sulfate—formation. To directly visualize the temporal evolution of sulfur-containing surface species, we further provide time-dependent in situ FTIR spectra as new panels (Figure 8b–d). As shown in Figure 8b–d, the sulfate-related bands (around 1189 and 1128 cm^{-1}) increase progressively with exposure time (0–15 min) and eventually approach a quasi-plateau, suggesting gradual accumulation of surface sulfate species followed by a slowing net formation rate as surface coverage and/or product-layer thickness increases. The growth is markedly accelerated in the presence of O_2 and is further enhanced by H_2O, consistent with promoted oxidation and hydrated-sulfate build-up under humid conditions. This time-dependent build-up provides molecular-level evidence supporting the faster transition toward mass-transfer limitation under $SO_2 + O_2 + H_2O$. From the time-resolved FTIR perspective, the progressive increase in the sulfate-related bands in the 1200–1100 cm^{-1} region (assigned to SO_4^{2-} species) reflects the ongoing sulphur mineralization on the external surface and near-surface region; the approach to a steady signal indicates that the net mineralization rate slows and tends toward a quasi-plateau as surface coverage/product-layer thickness increases. The presence of O_2 increases the mineralization rate by accelerating sulfite-to-sulfate conversion, whereas H_2O further promotes the formation of hydrated sulfate (e.g., $CaSO_4 \cdot 2H_2O$), leading to faster sulfate-band growth but also a more rapid buildup of diffusion-limiting deposits at pore mouths. In contrast, NO can sustain the effective mineralization rate for a longer period via NO/NO_2 redox cycling that continuously catalyzes sulfite oxidation, which is consistent with the extended durability observed in the fixed-bed tests. In the time domain, the sulfate-related bands (around 1189 and 1128 cm^{-1}) increase progressively with exposure time and eventually approach a plateau, indicating the gradual accumulation of surface sulfate species. The growth is markedly accelerated in the presence of O_2 and further enhanced by H_2O, consistent with promoted sulfite oxidation and the formation of hydrated sulfate. This time-dependent buildup also explains the faster transition to mass-transfer limitation under humid conditions due to accelerated product-layer coverage/densification. Importantly, the stronger sulfate bands

under humid conditions reconcile with the previously observed shorter sorbent lifetime: water accelerates product formation and surface coverage (hence stronger FTIR signals and the gypsum phase in XRD), yet simultaneously speeds up pore-mouth deposition and layer densification, increasing diffusion resistance and causing faster efficiency decay (consistent with SEM evidence). The carbonate region (≈1470–1420 cm^{-1}) shows no pronounced changes, suggesting that sulfate species dominate the surface chemistry under these atmospheres and temperatures. Overall, the in situ FTIR confirms at the molecular level that O_2 enhances the surface oxidation pathway while H_2O enhances hydrated-sulfate coverage; their combined effect yields stronger sulfate signatures but also aligns with faster mass-transfer limitation and deactivation, coherently supporting the XRD/SEM/BET and kinetic findings.

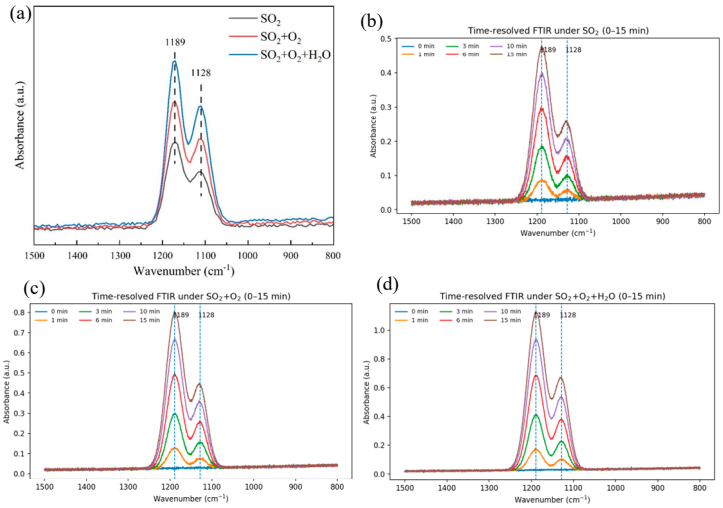


Figure 8. (**a**) In situ infrared spectra of desulfurization in different flue gases; Time-resolved in situ FTIR spectra during desulfurization under (**b**) SO_2, (**c**) SO_2 + O_2, (**d**) SO_2 + O_2 + H_2O (0–15 min).

4. Conclusions

In this work, a novel $Ca(OH)_2$-modified white mud sorbent was successfully developed and systematically evaluated for flue gas desulfurization, providing both a new utilization pathway for industrial solid waste and an effective material for SO_2 removal. Through optimization of preparation parameters, the most favorable conditions were determined to be a $Ca(OH)_2$-to-white mud mass ratio of 1:1, a thermal modification temperature of 60 °C, a treatment time of 6 h, and a liquid-to-solid ratio of 3:1. Under these conditions, the modified sorbent exhibited outstanding performance, achieving nearly complete SO_2 removal in the early reaction stage and maintaining efficiencies above 90% after 10 h, clearly outperforming either raw white mud or $Ca(OH)_2$ alone.

Comprehensive physicochemical characterizations revealed that the superior activity and durability originated from the synergistic combination of abundant basic active sites and a stable hierarchical pore structure. BET analysis confirmed that the modified sorbent possessed a significantly increased specific surface area and pore volume, which were largely retained after desulfurization, indicating high structural stability against pore blockage. SEM observations further demonstrated that the sorbent underwent a transformation from porous aggregates to product-layer densification, validating a porous-product-layer shrinking-core mechanism in which mass transfer resistance progressively dominates at later stages. XRD results confirmed the conversion of $CaCO_3$ into $CaSO_4 \cdot 2H_2O$ as the main reaction product, while in situ FTIR studies clarified the roles of gas components: O_2 promoted sulfite oxidation, H_2O accelerated hydrated sulfate formation, and NO/NO_2 redox cycling effectively extended sorbent lifetime by continuously catalyzing sulfite oxida-

tion. These molecular-level insights coherently supported the macroscopic desulfurization performance trends.

Overall, this study demonstrates that $Ca(OH)_2$-modified white mud combines high SO_2 removal efficiency, long-term stability, and strong structural resistance to deactivation, making it a promising alternative to conventional limestone-based sorbents. Beyond advancing the resourceful utilization of paper industry waste, the findings provide mechanistic insights and process guidance for the rational design of next-generation calcium-based sorbents with improved efficiency and durability. This work thus contributes not only to flue gas pollution control but also to the broader goals of industrial waste valorization and sustainable environmental management. Given that SO_2 removal proceeds mainly via conversion to gypsum ($CaSO_4 \cdot 2H_2O$), the spent sorbent is more suitably managed through byproduct utilization rather than chemical regeneration. Future work will quantify cyclic performance and assess practical routes for physical reactivation and gypsum-product valorization.

Author Contributions: Conceptualization, H.W. and Y.W.; methodology, J.W.; validation, C.X., L.Y. and L.J.; formal analysis, H.Y.; investigation, Y.G.; data curation, D.P.; writing—original draft preparation, H.W.; writing—review and editing, W.L.; All authors have read and agreed to the published version of the manuscript.

Funding: This research was funded by the East China Electric Power Test & Research Institute, China Datang Corporation Science and Technology General Research Institute Co., Ltd., grant number 3612412225556.

Data Availability Statement: For privacy reasons, the data presented in this study are available on request from the corresponding author.

Acknowledgments: This work was supported by the project of East China Electric Power Test & Research Institute, China Datang Corporation Science and Technology General Research Institute Co., Ltd.

Conflicts of Interest: Authors H.W., J.W., Y.W. and C.X. were employed by the company Datang Environment Industry Group Co., Ltd., and that authors L.J., W.L., H.Y. and Y.G. were employed by the company China Datang Corporation Science and Technology General Research Institute Co., Ltd. The remaining authors declare that the research was conducted in the absence of any commercial or financial relationships that could be construed as a potential conflict of interest. The Datang Environment Industry Group Co., Ltd. and China Datang Corporation Science and Technology General Research Institute Co., Ltd. had no role in the design of the study; in the collection, analyses, or interpretation of data; in the writing of the manuscript, or in the decision to publish the results.

References

1. Zhu, C.; Ru, J.; Gao, S.; Li, C. The simultaneous removal of NOx and SO_2 from flue gas by direct injection of sorbents in furnace of waste incinerator. *Fuel* **2023**, *333*, 126464. [CrossRef]
2. Wang, Y.; Wang, Z.; Liu, Y. Review on removal of SO_2, NOx, mercury, and arsenic from flue gas using green oxidation absorption technology. *Energy Fuels* **2021**, *35*, 9775–9794. [CrossRef]
3. Liu, C.; Shao, L.; Pan, C.; Wu, Z.; Wang, T.; Teng, W.; Chen, Y.; Zheng, C.; Gao, X. Ammonia-based post-combustion CO_2 and SO_2 integrating capture using multi-stage solvent circulation process. *Sep. Purif. Technol.* **2024**, *339*, 126611. [CrossRef]
4. Jędrusik, M.; Łuszkiewicz, D.; Świerczok, A.; Gostomczyk, M.; Kobylańska-Pawliszet, M. Simultaneous removal of NOx, SO_2, and Hg from flue gas in FGD absorber with oxidant injection ($NaClO_2$)–full-scale investigation. *J. Air Waste Manag. Assoc.* **2020**, *70*, 629–640. [CrossRef]
5. Rizwan, M.; Ali, M.F.; Nawaz, M.A.; He, M.; Song, Y.; Jiang, P.; Ullah, S.; Hassan, M.; Zhou, X. Exploring the synergistic effect of NaOH/NaClO absorbent in a novel wet FGD scrubber to control SOx/NOx emissions. *Environ. Monit. Assess.* **2025**, *197*, 170. [CrossRef]
6. Subah, K.; Abdullah, B.; Tahir, D. Innovations in calcium carbonate-based sorbents for SO_2 removal: Challenges and future prospects. *Int. J. Environ. Sci. Technol.* **2025**, *22*, 16181–16226. [CrossRef]

7. Xing, G.; Wang, W.; Zhao, S.; Qi, L. Application of Ca-based adsorbents in fixed-bed dry flue gas desulfurization (FGD): A critical review. *Environ. Sci. Pollut. Res.* **2023**, *30*, 76471–76490. [CrossRef]
8. Zacharczuk, W.; Andruszkiewicz, A.; Tatarek, A.; Alahmer, A.; Alsaqoor, S. Effect of Ca-based additives on the capture of SO_2 during combustion of pulverized lignite. *Energy* **2021**, *231*, 120988. [CrossRef]
9. Jeong, T.S.; Oh, M.K.; Chung, Y.; Park, J. Effect of white mud addition on desulfurization rate of molten steel. *Metall. Mater. Trans. B* **2021**, *52*, 3596–3605. [CrossRef]
10. Meng, H.; Wang, J.; Zhang, L.; Jin, K.; Liu, X.; Zhou, H. A new disposal method for white mud: Replacing limestone in iron ore sintering. *J. Environ. Manag.* **2023**, *348*, 119331. [CrossRef]
11. Bai, Y.; Chen, M.; Li, Q.; Huang, Y. Sulfation performance of CaO under circulating fluidized bed combustion-like condition. *J. Therm. Anal. Calorim.* **2020**, *142*, 1031–1042. [CrossRef]
12. Bu, L.; Sun, R.; Guan, Y.; Fang, C.; Ge, Z.; Ran, Y.; Zhang, H. Effect of white mud on carbonation resistance of alkali activated slag. *Constr. Build. Mater.* **2024**, *438*, 137207. [CrossRef]
13. Marques, L.; Mota, S.; Teixeira, P.; Mateus, M.; Pinheiro, C. Decarbonisation of cement industry: Calcium looping with white mud and limestone as CaO-based sorbents for industrial flue gas treatment. *Chem. Eng. Process. Process Intensif.* **2025**, *213*, 110290. [CrossRef]
14. Sun, R.; Bu, L.; Zhang, H.; Guan, Y.; Ma, C.; Ge, Z.; Šavija, B. Effect of white mud on properties of alkali activated slag. *Constr. Build. Mater.* **2023**, *392*, 131944. [CrossRef]
15. Sun, R.; Fang, C.; Zhang, H.; Ling, Y.; Feng, J.; Qi, H.; Ge, Z. Chemo-mechanical properties of alkali-activated slag/fly ash paste incorporating white mud. *Constr. Build. Mater.* **2021**, *291*, 123312. [CrossRef]
16. Zhu, M.-X.; Lee, L.; Wang, H.-H.; Wang, Z. Removal of an anionic dye by adsorption/precipitation processes using alkaline white mud. *J. Hazard. Mater.* **2007**, *149*, 735–741. [CrossRef]
17. Li, C.; Li, Y.; Zhang, C.; Chu, Z.; Fang, Y. Ca3B2O6-modified papermaking white mud for $CaCO_3$/CaO thermochemical energy storage. *Chem. Eng. J.* **2023**, *461*, 142096. [CrossRef]
18. Li, B.; Wu, H.; Liu, X.; Zhu, T.; Liu, F.; Zhao, X. Simultaneous removal of SO_2 and NO using a novel method with red mud as absorbent combined with O_3 oxidation. *J. Hazard. Mater.* **2020**, *392*, 122270. [CrossRef]
19. Jia, L.; Li, Z.; Yu, Q.; Gao, J.; Liu, C.; Liu, T.; Ning, P.; Wang, F. Removal of SO_2 and NOx from flue gas using mud-phosphorus slurry. *Environ. Sci. Pollut. Res.* **2020**, *27*, 23270–23280. [CrossRef]
20. Liu, Y.; Li, B.; Lei, X.; Liu, S.; Zhu, H.; Ding, E.; Ning, P. Novel method for high-performance simultaneous removal of NOx and SO_2 by coupling yellow phosphorus emulsion with red mud. *Chem. Eng. J.* **2022**, *428*, 131991. [CrossRef]
21. Zhang, X.; Liu, Z.; Wang, F.; Hu, S. Staged characteristics of red mud dealkalization by CO_2 and SO_2. *J. Clean. Prod.* **2023**, *411*, 137253. [CrossRef]
22. Nie, Z.; Zhao, Q.; Zhao, Q.; Li, Y.; Yang, D.; Liu, H.; Yang, S.; Li, J.; Tian, S.; Li, C.; et al. Red mud with enhanced dealkalization performance by supercritical water technology for efficient SO_2 capture. *J. Environ. Manag.* **2023**, *344*, 118469. [CrossRef]
23. Zhou, X.; Tang, W.; He, M.; Xiao, X.; Wang, T.; Cheng, S.; Zhang, L. Combined removal of SO_3 and HCl by modified $Ca(OH)_2$ from coal-fired flue gas. *Sci. Total Environ.* **2023**, *857*, 159466. [CrossRef]
24. Qi, L.; Luo, J.; Wang, W.; Zhao, W. Adsorption of SO_2 from sintering flue gas by alkali modified fly ash in electrostatic precipitator. *Sep. Sci. Technol.* **2023**, *58*, 1237–1251. [CrossRef]
25. Xuan, Y.; Peng, S.; Tian, H.; Hu, Z.; Yin, Y.; Gao, H. Selection of High-Performance Sorbent for H_2S Removal and Regulation of Reaction Products via Thermodynamic Simulation. *Materials* **2025**, *18*, 2918. [CrossRef] [PubMed]
26. Yan, D.; Zhu, Y.; Zhao, J.; Zhang, Q.; Wang, Y.; Yang, S. Synthesis and utilization of polyol-modified high specific surface area $Ca(OH)_2$: An investigation. *Environ. Sci. Pollut. Res.* **2024**, *31*, 32714–32724. [CrossRef] [PubMed]

Disclaimer/Publisher's Note: The statements, opinions and data contained in all publications are solely those of the individual author(s) and contributor(s) and not of MDPI and/or the editor(s). MDPI and/or the editor(s) disclaim responsibility for any injury to people or property resulting from any ideas, methods, instructions or products referred to in the content.